Design of Phase Codes for Radar Performance Optimization With a Similarity Constraint

Antonio De Maio, Silvio De Nicola, Yongwei Huang, Zhi-Quan Luo, Shuzhong Zhang

Abstract

This paper deals with the design of coded waveforms which optimize radar performances in the presence of colored Gaussian disturbance. We focus on the class of phase coded pulse trains and determine the radar code which approximately maximizes the detection performance under a similarity constraint with a pre-fixed radar code. This is tantamount to forcing a similarity between the ambiguity functions of the devised waveform and of the pulse train encoded with the pre-fixed sequence. We consider the cases of both continuous and finite phase alphabet, and formulate the code design in terms of a non-convex, NP-hard quadratic optimization problem. In order to approximate the optimal solutions, we propose techniques (with polynomial computational complexity) based on the method of Semidefinite Program (SDP) relaxation and randomization. Moreover, we also derive approximation bounds yielding a "measure of goodness" of the devised algorithms. At the analysis stage, we assess the performance of the new encoding techniques both in terms of detection performance and ambiguity function, under different choices for the similarity parameter. We also show that the new algorithms achieve an accurate approximation of the optimal solution with a modest number of randomizations.

Antonio De Maio and Silvio De Nicola are with Università degli Studi di Napoli "Federico II", Dipartimento di Ingegneria Elettronica e delle Telecomunicazioni, Via Claudio 21, I-80125 Napoli, Italy. E-mail: ademaio@unina.it, silviodenicola@gmail.com. This work has been performed during the visit of Antonio De Maio and Silvio De Nicola at the Department of Systems Engineering and Engineering Management of the Chinese University of Hong Kong.

Yongwei Huang and Shuzhong Zhang are with Department of Systems Engineering and Engineering Management, The Chinese University of Hong Kong, Shatin, Hong Kong. E-mail: ywhuang@se.cuhk.edu.hk, zhang@se.cuhk.edu.hk. The research of these authors is supported in part by Hong Kong RGC Earmarked Grants CUHK418505 and CUHK418406.

Z.-Q. Luo is with Department of Electrical and Computer Engineering, University of Minnesota. E-mail: luozq@ece.umn.edu. The research of this author is supported in part by the National Science Foundation, Grant No. DMS-0312416.

Index Terms

Radar Signal Processing, Non-Convex Quadratic Optimization, Semidefinite Program Relaxation and Randomization.

I. INTRODUCTION

The problem of radar waveform design has recently received a noticeable attention from the signal processing community. The invention of new flexible waveform generators and of high speed signal processing hardware has determined the development of advanced and often very sophisticated algorithms for radar signal shaping [1], [2].

Waveform optimization in the presence of colored disturbance with known covariance matrix has been addressed in [3]. Three techniques based on the maximization of the Signal to Noise Ratio (SNR) are introduced and analyzed. Two of them also exploit the degrees of freedom provided by a rank deficient disturbance covariance matrix. In [4], a signal design algorithm relying on the maximization of the SNR under a similarity constraint with a given waveform is proposed and assessed. The solution potentially emphasizes the target contribution and de-emphasizes the disturbance, preserving also some characteristics of the desired waveform. In [5] a signal subspace framework, which allows the derivation of the optimal radar waveform (in the sense of maximizing the SNR at the output of the detector) for a given scenario, is presented under the Gaussian assumption for the statistics of both the target and the clutter. Signal shaping for target matched-illumination has been considered in [6]-[10]. Moreover, further very recent and advanced techniques for radar waveform design can be found in [2] and references therein.

A quite different signal design approach relies on the modulation of a pulse train parameters (amplitude, phase, and frequency) in order to synthesize waveforms with some specified properties. This technique is known as the radar coding and a substantial bulk of work is nowadays available in the literature about this topic. Here we mention Barker, Frank, and Costas codes which lead to waveforms whose ambiguity functions share good resolution properties both in range and Doppler. This list is not exhaustive and a comprehensive treatment can be found in [11], [12]. Nevertheless, it is worth pointing out that the ambiguity function is not the only relevant objective function for code design in operating situations where the disturbance is not white. This might be the case of optimum radar detection in the presence of colored disturbance,

where the standard matched filter is no longer optimum and the most powerful radar receiver requires whitening operations.

In [13], focusing on the class of linearly coded pulse trains (both in amplitude and in phase), the authors propose a code selection algorithm which maximizes the detection performance but, at the same time, is capable of controlling both the region of achievable values for the Doppler estimation accuracy and the degree of similarity with a pre-fixed radar code. The algorithm first relaxes the original problem into a convex one which belongs to the SDP class; then it derives an optimum code through a rank-one decomposition of an optimal solution of the relaxed problem.

Nevertheless, in several practical situations, the radar amplifiers usually work in saturation conditions and hence an amplitude modulation might be difficult (even if not impossible) to perform. To this end, in the present paper, we focus on constant modulus waveform and consider the synthesis of phase coding schemes for radar coherent pulse trains. We study the cases of both continuous and finite phase alphabet, and formulate the code design in terms of a non-convex, NP-hard, quadratic optimization problem. In order to approximate the optimal solutions, we propose techniques (with polynomial computational complexity) based on SDP relaxation and randomization[1]. We also evaluate, in both the considered cases, the approximation bound which represents a "measure of goodness" of an approximation technique as it characterizes the quality of the solutions produced by the method. At the analysis stage, we assess the performance of the new encoding algorithms both in terms of detection capabilities and ambiguity function. The results show that they achieve an accurate approximation of the optimal solution with a quite modest number of randomizations. Moreover, depending on the design constraints, it is possible to trade off detection performance for desirable properties of the waveform ambiguity function.

The paper is organized as follows. In Section II, we present the model for both the transmitted and the received coded signal. In Section III, we discuss the criteria exploited for phase code design. In Sections IV and V, we introduce the new algorithms and derive the approximation bounds with reference to the cases of both continuous and finite code alphabet. In Section VI, we assess the performance of the proposed encoding methods also in comparison with standard radar codes. Finally, in Section VII, we draw conclusions and outline possible future research

[1]SDP relaxation and randomization techniques have also been used in other signal processing fields. For instance in maximum likelihood multiuser detection [14], Multiple Input Multiple Output (MIMO) decoding [15], and transmit beamforming [16].

tracks.

II. System Model

We consider a radar system which transmits a phase coded coherent burst of pulses

$$s(t) = a_t u(t) \exp[j(2\pi f_0 t + \phi)] \,,$$

where a_t is the transmit signal amplitude, $j = \sqrt{-1}$,

$$u(t) = \sum_{i=0}^{N-1} a(i) p(t - iT_r) \,,$$

is the signal's complex envelope (see Figure 1), $p(t)$ is the signature of the transmitted pulse, T_r is the Pulse Repetition Time (PRT), $[a(0), a(1), \ldots, a(N-1)] \in \mathbb{C}^N$ is the radar phase code (i.e. $a(i) = \exp[j\phi_i]$, $i = 0, \ldots, N-1$), f_0 is the carrier frequency, and ϕ is a random phase. Moreover, the pulse waveform $p(t)$ is of duration $T_p \leq T_r$ and has unit energy, i.e.

$$\int_0^{T_p} |p(t)|^2 dt = 1 \,,$$

where $|\cdot|$ denotes the modulus of a complex number. The signal backscattered by a target with a two-way time delay τ and received by the radar is

$$r(t) = \alpha_r e^{j2\pi(f_0 + f_d)(t-\tau)} u(t - \tau) + n(t) \,,$$

where α_r is the complex echo amplitude (accounting for the transmit amplitude, phase, target reflectivity, and channels propagation effects), f_d is the target Doppler frequency, and $n(t)$ is additive disturbance due to clutter and thermal noise.

This signal is down-converted to baseband and filtered through a linear system with impulse response $h(t) = p^*(-t)$, where $(\cdot)^*$ denotes complex conjugate. Let the filter output be

$$v(t) = \alpha_r e^{-j2\pi f_0 \tau} \sum_{i=0}^{N-1} a(i) e^{j2\pi i f_d T_r} \chi_p(t - iT_r - \tau, f_d) + w(t) \,,$$

where $\chi_p(\lambda, f)$ is the pulse waveform ambiguity function [11], i.e.

$$\chi_p(\lambda, f) = \int_{-\infty}^{+\infty} p(\psi) p^*(\psi - \lambda) e^{j2\pi f \psi} d\psi,$$

and $w(t)$ is the down-converted and filtered disturbance component. The signal $v(t)$ is sampled at $t_k = \tau + kT_r$, $k = 0, \ldots, N-1$, providing the observables[2]

$$v(t_k) = \alpha a(k) e^{j2\pi k f_d T_r} \chi_p(0, f_d) + w(t_k), \qquad k = 0, \ldots, N-1\,,$$

where $\alpha = \alpha_r e^{-j2\pi f_0 \tau}$. Since $\chi(0, f_d)$ does not depend on $a(k)$'s and, as a consequence, does not affect the design of radar code, we assume hereafter that $\chi(0, f_d) = 1$ for convenience. Hence, we can rewrite the samples $v(t_k)$ as

$$v(t_k) = \alpha a(k) e^{j2\pi k f_d T_r} + w(t_k), \qquad k = 0, \ldots, N-1\,.$$

Moreover, denoting by $\boldsymbol{c} = [a(0), a(1), \ldots, a(N-1)]^T$ the N-dimensional column vector containing the code elements[3], $\boldsymbol{p} = [1, e^{j2\pi f_d T_r}, \ldots, e^{j2\pi(N-1) f_d T_r}]^T$ the temporal steering vector, $\boldsymbol{v} = [v(t_0), v(t_1), \ldots, v(t_{N-1})]^T$, and $\boldsymbol{w} = [w(t_0), w(t_1), \ldots, w(t_{N-1})]^T$, we get the following vectorial model for the backscattered signal

$$\boldsymbol{v} = \alpha \boldsymbol{c} \odot \boldsymbol{p} + \boldsymbol{w}\,, \tag{1}$$

where $\odot$ denotes the Hadamard element-wise product [17].

III. Radar Phase Code Design Criteria

As already said in the introduction, we are looking for the phase code which optimizes the detection performance, under a similarity constraint with a given radar code exhibiting a good ambiguity function. In this section, we formulate mathematically the aforementioned criterion highlighting how the detection probability can be maximized and the similarity constraint can be enforced. To this end, we recall that the problem of detecting a target in the presence of observables described by the model (1) can be formulated in terms of the following binary hypotheses test

$$\begin{cases} H_0: \ \boldsymbol{v} = \boldsymbol{w} \\ \\ H_1: \ \boldsymbol{v} = \alpha \boldsymbol{c} \odot \boldsymbol{p} + \boldsymbol{w} \end{cases}. \tag{2}$$

[2]We neglect range straddling losses and also assume that there are no target range ambiguities. This last assumption is usually met in Low Pulse Repetition Frequency (LPRF) radars (and in particular in medium-long range radars for early warning applications), but might be restrictive for High PRF (HPRF) systems.

[3]$(\cdot)^T$ is the transpose operator.

We assume that the disturbance vector $\boldsymbol{w}$ is a zero-mean complex circular Gaussian vector with known positive definite covariance matrix

$$E[\boldsymbol{w}\boldsymbol{w}^{\dagger}] = \boldsymbol{M}$$

($E[\cdot]$ denotes mathematical expectation and $(\cdot)^{\dagger}$ conjugate transpose). This implies that the Generalized Likelihood Ratio Test (GLRT) detector for the problem (2), which coincides with the optimum test [18] (according to the Neyman-Pearson criterion) if the phase of α is uniformly distributed in $[0, 2\pi)$, is given by

$$|\boldsymbol{v}^{\dagger}\boldsymbol{M}^{-1}(\boldsymbol{c} \odot \boldsymbol{p})|^2 \underset{H_0}{\overset{H_1}{\gtrless}} G\,, \tag{3}$$

where G is the detection threshold set according to a desired value of the false alarm Probability (P_{fa}). An analytical expression of the detection Probability (P_d), for a given value of P_{fa}, is available for both the cases of non-fluctuating and fluctuating target. In the former case (NFT),

$$P_d = Q\left(\sqrt{2|\alpha|^2(\boldsymbol{c} \odot \boldsymbol{p})^{\dagger}\boldsymbol{M}^{-1}(\boldsymbol{c} \odot \boldsymbol{p})}, \sqrt{-2\ln P_{fa}}\right), \tag{4}$$

while, for the case of Rayleigh fluctuating target (RFT) with $E[|\alpha|^2] = \sigma_a^2$,

$$P_d = \exp\left(-\frac{\ln P_{fa}}{1 + \sigma_a^2(\boldsymbol{c} \odot \boldsymbol{p})^{\dagger}\boldsymbol{M}^{-1}(\boldsymbol{c} \odot \boldsymbol{p})}\right), \tag{5}$$

where $Q(\cdot,\cdot)$ denotes the Marcum Q function of order 1. These last expressions show that, given P_{fa}, P_d depends on the radar code, the disturbance covariance matrix and the temporal steering vector only through the SNR, defined as

$$\text{SNR} = \begin{cases} |\alpha|^2(\boldsymbol{c} \odot \boldsymbol{p})^{\dagger}\boldsymbol{M}^{-1}(\boldsymbol{c} \odot \boldsymbol{p}) & \text{NFT} \\ \\ \sigma_a^2(\boldsymbol{c} \odot \boldsymbol{p})^{\dagger}\boldsymbol{M}^{-1}(\boldsymbol{c} \odot \boldsymbol{p}) & \text{RFT} \end{cases} \tag{6}$$

Moreover, P_d is an increasing function of SNR and, as a consequence, the maximization of P_d can be obtained maximizing the quadratic form

$$(\boldsymbol{c} \odot \boldsymbol{p})^{\dagger}\boldsymbol{M}^{-1}(\boldsymbol{c} \odot \boldsymbol{p}) = \boldsymbol{c}^{\dagger}\boldsymbol{R}\boldsymbol{c}\,, \tag{7}$$

where $\boldsymbol{R} = \boldsymbol{M}^{-1} \odot (\boldsymbol{p}\boldsymbol{p}^{\dagger})^{*}$, over the radar code. We just highlight that $\boldsymbol{R}$ is the Hadamard product of two positive semidefinite matrices, and hence $\boldsymbol{R}$ is itself positive semidefinite [19, p. 1352, A.77].

If the maximization of (7) is performed under only an energy constraint for the transmitted vector (i.e. $\|\boldsymbol{c}\|^2 = N$, where $\|\cdot\|$ denotes the Euclidean norm of a complex vector), the optimum code is proportional to the eigenvector of $\boldsymbol{R}$ corresponding to the largest eigenvalue. Unfortunately, this solution does not usually belong to the class of phase codes and, even if it provides the best detection performance, it does not usually exhibit good ambiguity properties (i.e. a narrow main peak both in range and in Doppler and relatively low sidelobe peaks). Enforcing a similarity constraint with a given phase code $\boldsymbol{c}_0$, which shares a good ambiguity, seems a reasonable way to optimize P_d and, at the same time, of controlling the ambiguity distortion. This is tantamount to optimizing the detection performance in a suitable neighborhood of a known code, where the ambiguity function exhibits acceptable behavior. In this paper we exploit the l_∞ norm[4] to impose the similarity, namely we force

$$||\boldsymbol{c} - \boldsymbol{c}_0||_\infty \leq \epsilon,$$

where $0 \leq \epsilon \leq 2$ is a real parameter ruling the degree of similarity. We also consider two possibilities for the entries of $\boldsymbol{c}$. The former just assumes that $\boldsymbol{c}$ is a phase code, namely the modulus of the k-th entry $|\boldsymbol{c}(k)| = 1$, $k = 1, \ldots, N$. The latter considers the case of a finite code alphabet of size M, i.e. $\boldsymbol{c}(k) \in \{1, e^{j2\pi\frac{1}{M}}, \ldots, e^{j2\pi\frac{M-1}{M}}\}$, $k = 1, \ldots, N$. In this last situation, we also suppose that the entries of the similarity code belong to the same alphabet as the sought vector. In the next two sections, we introduce phase coding algorithms for each of the aforementioned situations.

IV. Phase Coding Algorithm with Similarity Constraint (PCA-SC)

In this section, we focus on the case $|\boldsymbol{c}(k)| = 1$, $k = 1, \ldots, N$, and formulate the phase code design in terms of the following complex quadratic optimization problem

$$\begin{aligned} \max \quad & \boldsymbol{c}^\dagger \boldsymbol{R} \boldsymbol{c} \\ \text{s.t.} \quad & ||\boldsymbol{c} - \boldsymbol{c}_0||_\infty \leq \epsilon, \\ & |\boldsymbol{c}(k)| = 1, \qquad k = 1, \ldots, N\,, \end{aligned} \tag{8}$$

where the parameter ϵ rules the set of admissible codes. Specifically, decreasing ϵ is tantamount to reducing the size of the feasible region. The similarity constraint in (8) can be equivalently

[4]Given an N-dimensional complex vector $\boldsymbol{x}$ its l_∞ norm [17] is defined as $||\boldsymbol{x}||_\infty = \max_{k\in(1,\ldots,N)} |\boldsymbol{x}(k)|$.

written[5] as $|\boldsymbol{c}(k) - \boldsymbol{c}_0(k)| \leq \epsilon$, or $\Re\left[\boldsymbol{c}^*(k)\boldsymbol{c}_0(k)\right] \geq 1 - \epsilon^2/2$, for $k = 1, \ldots, N$, which implies $\arg \boldsymbol{c}(k) \in [\gamma_k, \gamma_k + \delta_c]$, where $\gamma_k = \arg \boldsymbol{c}_0(k) - \arccos(1 - \epsilon^2/2)$ and $\delta_c = 2\arccos\left(1 - \epsilon^2/2\right)$ for $k = 1, \ldots, N$. Based on this observation, problem (8) can be recast as

$$\begin{aligned} \max \quad & \boldsymbol{c}^\dagger \boldsymbol{R}\boldsymbol{c} \\ \text{s.t.} \quad & \arg \boldsymbol{c}(k) \in [\gamma_k, \gamma_k + \delta_c]\,, \\ & |\boldsymbol{c}(k)| = 1, \qquad k = 1, \ldots, N\,. \end{aligned} \tag{9}$$

Notice that in the instance of $\epsilon = 2$ (or equivalently $\delta_c = 2\pi$), the phase constraints of (9) are redundant and the problem reduces to

$$\begin{aligned} \max \quad & \boldsymbol{c}^\dagger \boldsymbol{R}\boldsymbol{c} \\ \text{s.t.} \quad & |\boldsymbol{c}(k)| = 1, \qquad k = 1, \ldots, N\,. \end{aligned} \tag{10}$$

Even the simpler formulation (10) is NP-hard [20], [21], but there exist efficient approximation algorithms, based on relaxation and randomization, which achieve an accurate approximation of the optimal solution with a modest number of randomizations [21], [22].

According to the NP-hard nature of problem (9), one cannot find polynomial time algorithms for computing its optimal solutions. As a consequence, in the following, we focus on approximation techniques and propose the following relaxation and randomization algorithm which provides a randomized feasible solution of (9).

Algorithm I: PCA-SC

1) Solve the SDP problem below and denote by $\hat{\boldsymbol{Z}}$ an optimal solution:

$$\begin{aligned} \text{(SDP)} \quad \max \quad & \operatorname{tr}(\boldsymbol{R}\boldsymbol{Z}) \\ \text{s.t.} \quad & \boldsymbol{Z}_{kk} = 1, \qquad k = 1, \ldots, N, \\ & \boldsymbol{Z} \succeq 0 \end{aligned}$$

($\boldsymbol{Z}_{kk}$ denotes the (k,k)-th entry of $\boldsymbol{Z}$ and $\boldsymbol{Z} \succeq 0$ indicates that $\boldsymbol{Z}$ is positive semidefinite).

2) Generate a random vector $\boldsymbol{\xi} \in \mathbb{C}^N$ from the complex normal distribution $\mathcal{N}_{\mathbb{C}}(0, \boldsymbol{Y})$ where $\boldsymbol{Y} = \hat{\boldsymbol{Z}} \odot \boldsymbol{y}_c\boldsymbol{y}_c^\dagger$, where $\boldsymbol{y}_c = [e^{-j\gamma_1}, \ldots, e^{-j\gamma_N}]^T$.

3) Assign each $\boldsymbol{c}(k) = \boldsymbol{y}_c^*(k)\sigma(\xi_k)$, $k = 1, \ldots, N$, where

$$\sigma(x) = e^{j\frac{\arg x}{2\pi}\delta_c}, x \in \mathbb{C}.$$

[5]Let x be a complex number, $\Re[x]$ is the real part of x, and $\arg x \in [0, 2\pi)$ denotes the phase of x.

We point out that, in order to improve the approximation quality, the randomization steps (2 and 3) are repeated several times, and the randomized feasible solution yielding the largest objective function will be chosen as the approximate solution. As it will be shown in the performance analysis, the proposed randomization can achieve an accurate approximation of the optimal solution with a quite modest number of randomizations.

As to the computational complexity connected with the implementation of the algorithm, the solution of the SDP relaxation requires $O(N^{3.5})$ floating point operations (flops)[6] whereas each randomization involves $O(N^2)$ flops [14]. It follows that, for a modest number of randomizations, the most relevant contribution to the computational is connected with the SDP solution.

Finally, we explicitly acknowledge that, at the current state of the art, most radar systems use phase coded waveforms, where the phases are taken from a finite and regularly spaced alphabet. This represents a limiting factor that prevents the practical realization of the PCA-SC. Nevertheless, even if the current technology is not able to implement on the field the proposed algorithm, it may not be definitely ruled out in the near future.

A. Approximation Bound

A "measure of goodness" of an approximation algorithm is provided by the approximation bound which characterizes the quality of the produced solutions. In the literature, a randomized approximation method for a maximization problem has an approximation bound (or performance guarantee, or worst case ratio) $R \in (0, 1]$, if for all instances of the problem, it always delivers a feasible solution whose expected value is at least R times the maximum value. Such an algorithm is usually called randomized R-approximation algorithm. More precisely, let $v(\cdot)$ be the maximum value of an instance of a given problem $(\cdot)$, then a feasible solution z produced by a randomized R-approximation algorithm, complies with

$$E[\text{the objective function evaluated at } z] \geq Rv(\cdot)\,.$$

It is clear that an algorithm produces a *better* approximation, if the approximation bound is *closer* to 1. In this subsection, we aim at establishing an approximation bound for Algorithm I.

[6]Herein, we use the usual Landau notation $O(n)$; hence, an algorithm is $O(n)$ if its implementation requires a number of flops proportional to n [23].

Theorem 4.1: Denoting by $\boldsymbol{z}$ an output of Algorithm I and by $v(\text{SDP})$ the optimal value of SDP, the following inequality holds true

$$E[\boldsymbol{z}^\dagger \boldsymbol{R}\boldsymbol{z}] \geq R_c v \text{ (SDP)}\,,$$

where

$$R_c = \frac{\pi(1-\cos\delta_c)}{2(2\pi-\delta_c)^2},$$

that is , Algorithm I has an approximation bound R_c.

Proof. Let $u_k = \frac{w^*}{4\sqrt{\pi}}\boldsymbol{y}_c^*(k)$, where w is the complex number

$$w = \frac{2\pi(-\sin\delta_c + j(1-\cos\delta_c))}{2\pi-\delta_c}\,.$$

To compute $E[\boldsymbol{z}(k)\boldsymbol{z}^*(l)]$, we exploit the equality

$$E[\boldsymbol{z}(k)\boldsymbol{z}^*(l)] = -u_k u_l^* E[\boldsymbol{\xi}(k)\boldsymbol{\xi}^*(l)] + u_k E[\boldsymbol{\xi}(k)\boldsymbol{z}^*(l)] +$$
$$u_l^* E[\boldsymbol{\xi}^*(l)\boldsymbol{z}(k)] + E[(u_k\boldsymbol{\xi}(k)-\boldsymbol{z}(k))(u_l\boldsymbol{\xi}(l)-\boldsymbol{z}(l))^*]. \quad (11)$$

We now evaluate the first three terms in the right-hand side of the above equality

(1) $-u_k u_l^* E[\boldsymbol{\xi}(k)\boldsymbol{\xi}^*(l)] = -\frac{1}{16\pi}|w|^2\hat{\boldsymbol{Z}}_{kl}$.

(2) $u_k E[\boldsymbol{\xi}(k)\boldsymbol{z}^*(l)] = \frac{1}{16\pi}|w|^2\hat{\boldsymbol{Z}}_{kl}$. Since

$$\begin{bmatrix} \boldsymbol{\xi}(k) \\ \boldsymbol{\xi}(l) \end{bmatrix} \in \mathcal{N}_{\mathbb{C}}\left(0, \begin{bmatrix} 1 & \boldsymbol{Y}_{kl} \\ \boldsymbol{Y}_{lk} & 1 \end{bmatrix}\right),$$

we may represent the components as

$$\boldsymbol{\xi}(k) = \boldsymbol{Y}_{kl}\eta + \sqrt{1-|\boldsymbol{Y}_{kl}|^2}\lambda, \boldsymbol{\xi}(l) = \eta, \begin{bmatrix} \eta \\ \lambda \end{bmatrix} \in \mathcal{N}_C\left(0, \begin{bmatrix} 1 & 0 \\ 0 & 1 \end{bmatrix}\right).$$

It follows that

$$\begin{aligned} E[\boldsymbol{\xi}(k)\boldsymbol{z}^*(l)] &= E[(\boldsymbol{Y}_{kl}\eta + \sqrt{1-|\boldsymbol{Y}_{kl}|^2}\lambda)\boldsymbol{y}_c(l)\sigma^*(\eta)] \\ &= \boldsymbol{Y}_{kl}\boldsymbol{y}_c(l)E[\eta\sigma^*(\eta)] + \sqrt{1-|\boldsymbol{Y}_{kl}|^2}\boldsymbol{y}_c(l)E[\lambda\sigma^*(\eta)] \\ &= \boldsymbol{Y}_{kl}\boldsymbol{y}_c(l)E[\eta\sigma^*(\eta)], \end{aligned}$$

where the statistical independence between η and λ is exploited in the last equality. Notice that

$$\begin{aligned} & E[\eta\sigma^*(\eta)] \\ = & \int_0^\infty \int_0^{2\pi} \rho e^{j\alpha}\sigma^*(\rho e^{j\alpha})\frac{\rho}{\pi}e^{-\rho^2}d\alpha d\rho \\ = & \int_0^\infty \int_0^{2\pi} \rho e^{j\alpha}\sigma^*(e^{j\alpha})\frac{\rho}{\pi}e^{-\rho^2}d\alpha d\rho \\ = & \frac{1}{\pi}\int_0^\infty \rho^2 e^{-\rho^2}d\rho \int_0^{2\pi} e^{j\alpha}\sigma^*(e^{j\alpha})d\alpha \\ = & \frac{1}{4\sqrt{\pi}}\int_0^{2\pi} e^{j\alpha}\sigma^*(e^{j\alpha})d\alpha \\ = & \frac{w}{4\sqrt{\pi}}, \end{aligned}$$

where we have used the polar coordinate representation $\eta = \rho e^{j\alpha}$ in the first equality, $\int_0^\infty \rho^2 e^{-\rho^2}d\rho = \frac{\sqrt{\pi}}{4}$ in the second last equality, and $\int_0^{2\pi} e^{j\alpha}\sigma^*(e^{j\alpha})d\alpha = w$ in the last equality. Therefore, we have

$$u_k E[\boldsymbol{\xi}(k)\boldsymbol{z}^*(l)] = u_k \boldsymbol{Y}_{kl}\boldsymbol{y}_c(l)\frac{w}{4\sqrt{\pi}} = \frac{1}{16\pi}|w|^2\hat{\boldsymbol{Z}}_{kl}.$$

(3) $u_l^* E[\boldsymbol{\xi}^*(l)\boldsymbol{z}(k)] = \frac{1}{16\pi}|w|^2\hat{\boldsymbol{Z}}_{kl}$.

Exploiting the representation

$$\boldsymbol{\xi}(k) = \eta, \boldsymbol{\xi}(l) = \boldsymbol{Y}_{kl}^*\eta + \sqrt{1-|\boldsymbol{Y}_{kl}|^2}\lambda, \left[\begin{array}{c} \eta \\ \lambda \end{array}\right] \in \mathcal{N}_{\mathbb{C}}\left(0, \left[\begin{array}{cc} 1 & 0 \\ 0 & 1 \end{array}\right]\right),$$

it can be shown that $u_l^* E[\boldsymbol{\xi}^*(l)\boldsymbol{z}(k)] = \frac{1}{16\pi}|w|^2\hat{\boldsymbol{Z}}_{kl}$.

It thus follows from (11) that

$$E[\boldsymbol{z}(k)\boldsymbol{z}^*(l)] = \frac{1}{16\pi}|w|^2\hat{\boldsymbol{Z}}_{kl} + E[(u_k\boldsymbol{\xi}(k) - \boldsymbol{z}(k))(u_l\boldsymbol{\xi}(l) - \boldsymbol{z}(l))^*].$$

Denoting by $\boldsymbol{s}$ the N-dimensional complex vector with entries $\boldsymbol{s}(k) = u_k\boldsymbol{\xi}(k) - \boldsymbol{z}(k)$, $k = 1, \ldots, N$, the above equality implies that

$$E[\boldsymbol{z}\boldsymbol{z}^\dagger] = \frac{1}{16\pi}|w|^2\hat{\boldsymbol{Z}} + E[\boldsymbol{s}\boldsymbol{s}^\dagger].$$

Now, since $\boldsymbol{R} \succeq 0$, we have

$$E[\boldsymbol{z}^\dagger\boldsymbol{R}\boldsymbol{z}] = E[\text{tr}(\boldsymbol{R}\boldsymbol{z}\boldsymbol{z}^\dagger)] = \frac{|w|^2}{16\pi}\text{tr}(\boldsymbol{R}\hat{\boldsymbol{Z}}) + E[\text{tr}(\boldsymbol{R}\boldsymbol{s}\boldsymbol{s}^\dagger)] \geq \frac{|w|^2}{16\pi}\text{tr}(\boldsymbol{R}\hat{\boldsymbol{Z}}) = \frac{|w|^2}{16\pi}v(\text{SDP}).$$

This completes the proof. □

It remains to show that $R_c \in (0,1)$. To this end, we claim that $R_c \in (0, \frac{\pi}{4}]$ for any given $\delta_c \in (0, 2\pi]$. This result stems from the following

Proposition 4.2: The univariate function

$$f(x) = \frac{\sqrt{2(1-\cos x)}}{2\pi - x}$$

is strictly increasing over $(0, 2\pi)$, and $f(0) = 0$, $f(2\pi) = 1$.

Proof. See Appendix A. □

We remark that the obtained approximation bound is independent of γ_k's. Further, as already pointed out, when $\delta_c = 2\pi$, namely phase constraints in (9) redundant, the bound is $\frac{\pi}{4}$ which agrees with the results of [21] and [22].

V. Finite Alphabet Phase Coding Algorithm with Similarity Constraint (FA-PCA-SC)

In this section, we focus on the finite alphabet case namely $\boldsymbol{c}(k) \in \{1, e^{j2\pi\frac{1}{M}}, \ldots, e^{j2\pi\frac{M-1}{M}}\}$, $k = 1, \ldots, N$, and formulate the design of the phase code in terms of the following complex quadratic optimization problem

$$\begin{aligned} \max \quad & \boldsymbol{c}^\dagger \boldsymbol{R} \boldsymbol{c} \\ \text{s.t.} \quad & ||\boldsymbol{c} - \boldsymbol{c}_0||_\infty \leq \epsilon, \\ & \boldsymbol{c}(k) \in \{1, e^{j2\pi\frac{1}{M}}, \ldots, e^{j2\pi\frac{M-1}{M}}\}, \qquad k = 1, \ldots, N \end{aligned} \tag{12}$$

where $\boldsymbol{c}_0(k) \in \{1, e^{j2\pi\frac{1}{M}}, \ldots, e^{j2\pi\frac{M-1}{M}}\}, k = 1, \ldots, N$, and $M \geq 3$.

Notice that the constraint $|\boldsymbol{c}(k) - \boldsymbol{c}_0(k)| \leq \epsilon$, $k = 1, \ldots, N$, is equivalent to $\Re\left[\boldsymbol{c}(k)\boldsymbol{c}_0^*(k)\right] \geq 1 - \epsilon^2/2$ for each k, which in turn amounts to enforcing

$$\boldsymbol{c}(k) \in \left\{e^{j2\pi\frac{\beta_k}{M}}, e^{j2\pi\frac{\beta_k+1}{M}}, \ldots, e^{j2\pi\frac{\beta_k+\delta_d-1}{M}}\right\},$$

where

$$\beta_k = \frac{M \arg(\boldsymbol{c}_0(k))}{2\pi} - \left\lfloor \frac{M \arccos(1-\epsilon^2/2)}{2\pi} \right\rfloor$$

depends on $\boldsymbol{c}_0(k)$ and ϵ,

$$\delta_d = \begin{cases} 1 + 2\lfloor \frac{M \arccos(1-\epsilon^2/2)}{2\pi} \rfloor & \epsilon \in [0, 2) \\ M & \epsilon = 2 \end{cases}$$

depends only on ϵ, and $\lfloor \cdot \rfloor$ denotes the integer floor operation. Based on this observation, problem (12) can be recast as

$$\begin{aligned} \max \quad & \boldsymbol{c}^\dagger \boldsymbol{R} \boldsymbol{c} \\ \text{s.t.} \quad & \arg \boldsymbol{c}(k) \in \tfrac{2\pi}{M} \left[\beta_k, \beta_k + 1, \ldots, \beta_k + \delta_d - 1\right], \\ & |\boldsymbol{c}(k)| = 1, \qquad k = 1, \ldots, N \end{aligned} \tag{13}$$

It can be exactly solved by an exhaustive search in which the objective function is evaluated for all possible combinations of the $\boldsymbol{c}(k)$'s ensuring feasibility. Nevertheless, this kind of search is prohibitive due to its exponentially increasing computational complexity (i.e. $O(M^N)$). Hence, it would be desirable to devise algorithms that could efficiently find (in polynomial time) the global optimal solution. Unfortunately, such algorithms do not exist because the considered problem is NP-hard. To clarify this point, we consider the special instance of redundant similarity constraints in (13), i.e. $\epsilon = 2$, where the problem reduces to

$$\begin{aligned} \max \quad & \boldsymbol{c}^\dagger \boldsymbol{R} \boldsymbol{c} \\ \text{s.t.} \quad & \boldsymbol{c}(k) \in \{1, e^{j2\pi\frac{1}{M}}, \ldots, e^{j2\pi\frac{M-1}{M}}\}, \qquad k = 1, \ldots, N \end{aligned} \tag{14}$$

Thus, we observe that (14) is NP-hard since it includes Max 3-Cut problems [24], [25] as special cases. Due to the NP-hard nature of (13), in the following we focus our attention to approximation algorithms sharing a polynomial computational complexity. Specifically, we propose the following relaxation and randomization algorithm which provides a randomized feasible solution of (13).

Algorithm II: FA-PCA-SC

1) Solve the SDP problem below and denote by $\hat{\boldsymbol{Z}}$ an optimal solution:

$$\begin{aligned} \text{(SDP)} \quad \max \quad & \text{tr}\,(\boldsymbol{R}\boldsymbol{Z}) \\ \text{s.t.} \quad & \boldsymbol{Z}_{kk} = 1, \qquad k = 1, \ldots, N, \\ & \boldsymbol{Z} \succeq 0. \end{aligned}$$

2) Generate a random vector $\boldsymbol{\xi} \in \mathbb{C}^N$ from the complex normal distribution $\mathcal{N}_{\mathbb{C}}(0, \boldsymbol{W})$ where $\boldsymbol{W} = \hat{\boldsymbol{Z}} \odot \boldsymbol{y}_d \boldsymbol{y}_d^{\dagger}$, where $\boldsymbol{y}_d = [e^{-j\frac{2\pi}{M}\beta_1}, \ldots, e^{-j\frac{2\pi}{M}\beta_N}]^T$,

3) Assign each $\boldsymbol{c}(k) = \boldsymbol{y}_d^*(k)\mu(\xi_k)$, where $\mu(x)$ is defined as

$$\mu(x) = \begin{cases} 1, & \text{if } \arg x \in [0, 2\pi\frac{1}{\delta_d}); \\ e^{j2\pi\frac{1}{M}}, & \text{if } \arg x \in [2\pi\frac{1}{\delta_d}, 2\pi\frac{2}{\delta_d}); \\ \vdots & \\ e^{j2\pi\frac{\delta_d - 1}{M}}, & \text{if } \arg x \in [2\pi\frac{\delta_d - 1}{\delta_d}, 2\pi). \end{cases}$$

As for the PCA-SC, the computational complexity is mostly related to the solution of the SDP problem ($O(N^{3.5})$ flops). Moreover, also with reference to the finite alphabet case, a modest number of randomizations is sufficient to ensure satisfactory performances.

A. Approximation Bound

In this subsection, we derive the approximation bound for Algorithm II. Precisely, we prove the following

Theorem 5.1: Denoting by $\boldsymbol{z}$ an output of Algorithm II and by v (SDP) the optimal value of SDP, the following inequality holds true

$$E[\boldsymbol{z}^{\dagger}\boldsymbol{R}\boldsymbol{z}] \geq R_d v \text{ (SDP)}\,,$$

where

$$R_d = \frac{\sin^2(\pi\frac{1}{\delta_d})\sin^2(\pi\frac{\delta_d}{M})}{4\pi\sin^2(\pi(\frac{1}{\delta_d} - \frac{1}{M}))}.$$

Namely, Algorithm II has an approximation bound R_d.

Proof. The proof can be done with the same technique as Theorem (4.1) replacing $\sigma(\cdot)$ with $\mu(\cdot)$, $\boldsymbol{Y}$ with $\boldsymbol{W}$, letting

$$w = j(1 - e^{j2\pi\frac{1}{\delta_d}})\frac{1 - e^{j2\pi\frac{\delta_d}{M}}}{e^{j2\pi\frac{\delta_d - 1}{M}}(e^{j2\pi\frac{1}{\delta_d}} - e^{j2\pi\frac{1}{M}})}\,,$$

and observing that

$$\begin{aligned}
&\int_0^{2\pi} e^{j\alpha}\mu^*(e^{j\alpha})d\alpha \\
= &\int_0^{2\pi\frac{1}{\delta_d}} e^{j\alpha}d\alpha + \int_{2\pi\frac{1}{\delta_d}}^{2\pi\frac{2}{\delta_d}} e^{j\alpha}e^{-j2\pi\frac{1}{M}}d\alpha + \cdots + \int_{2\pi\frac{\delta_d-1}{\delta_d}}^{2\pi} e^{j\alpha}e^{-j2\pi\frac{\delta_d-1}{M}}d\alpha \\
= &\ j(1-e^{j2\pi\frac{1}{\delta_d}}) + j(1-e^{j2\pi\frac{1}{\delta_d}})e^{-j2\pi\frac{1}{M}}e^{j2\pi\frac{1}{\delta_d}} + \cdots + j(1-e^{j2\pi\frac{1}{\delta_d}})e^{-j2\pi\frac{\delta_d-1}{M}}e^{j2\pi\frac{\delta_d-1}{\delta_d}} \\
= &\ j(1-e^{j2\pi\frac{1}{\delta_d}})(1+e^{-j2\pi\frac{1}{M}}e^{j2\pi\frac{1}{\delta_d}} + \cdots + e^{-j2\pi\frac{\delta_d-1}{M}}e^{j2\pi\frac{\delta_d-1}{\delta_d}}) \\
= &\ j(1-e^{j2\pi\frac{1}{\delta_d}})\frac{1-e^{j2\pi\frac{\delta_d}{M}}}{e^{j2\pi\frac{\delta_d-1}{M}}(e^{j2\pi\frac{1}{\delta_d}}-e^{j2\pi\frac{1}{M}})} \\
= &\ w.
\end{aligned}$$

□

It still remains to prove that $R_d \in (0,1)$. To this end, we claim that $R_d \in \left(0, \frac{M^2\sin^2(\pi\frac{1}{M})}{4\pi}\right]$ for any given $\delta_d \in (1, M]$. This result stems directly from the following

Proposition 5.2: The univariate function

$$f(x) = \frac{2\sin(\pi\frac{1}{x})\sin(\pi\frac{x}{M})}{\sin(\pi(\frac{1}{x}-\frac{1}{M}))}$$

is strictly increasing over $(1, M)$, and $f(1) = 0$, $f(M) = 2M\sin(\pi\frac{1}{M})$.

Proof. See Appendix B. □

We remark that, when δ_d is equal to M, namely inactive similarity constraint, the approximation bound is $\frac{M^2\sin^2(\pi\frac{1}{M})}{4\pi}$, which coincides with that derived in [21] and [22]. Moreover, $0 < \frac{M^2\sin^2(\pi\frac{1}{M})}{4\pi} \leq 1$ for any $M \geq 3$, and $\frac{M^2\sin^2(\pi\frac{1}{M})}{4\pi}$ tends to $\frac{\pi}{4}$ as M goes to infinity.

Let us just take a look at the case $M = 16$. The bound is $R = 0.7740$ if $\epsilon = 2$; $R = 0.7641$ if $\epsilon \in [1.9616, 2)$; $R = 0.6856$ if $\epsilon \in [1.8478, 1.9616)$; $R = 0.5497$ if $\epsilon \in [1.6629, 1.8478)$; $R = 0.3869$ if $\epsilon \in [1.4142, 1.6629)$; $R = 0.2310$ if $\epsilon \in [1.1111, 1.4142)$; $R = 0.1084$ if $\epsilon \in [0.7654, 1.1111)$; $R = 0.0326$ if $\epsilon \in [0.3902, 0.7654)$; if $\epsilon \in [0, 0.3902)$, then $\delta_d = 1$, i.e., the problem is trivial because it contains only one feasible solution.

Before concluding this section, it is necessary to highlight that an on-line waveform design might be computationally intensive especially for airborne applications. However, what we would remark is that the design of the code does not have to be done necessarily on-line. For instance,

one can construct (off-line) a codebook, based on some suitable a-priori covariance models, and just to select the element of the codebook. Further, the algorithm might be on-line applied to other kind of radars (not necessarily airborne), where the environment is not rapidly varying and there is sufficient time to perform the design of the code before a significant change in the operating conditions.

VI. Performance Analysis

The present section is aimed at analyzing the performance of the proposed encoding schemes. To this end we assume that the disturbance covariance matrix is exponentially shaped with one-lag correlation coefficient $\rho = 0.8$, i.e.

$$\boldsymbol{M}_{ij} = \rho^{|i-j|},$$

and fix P_{fa} of the receiver (3) to 10^{-6}. As to the temporal steering vector $\boldsymbol{p}$, we set[7] the normalized Doppler frequency $f_d T_r = 0.15$. The analysis is conducted in terms of both P_d and ambiguity function of the phase coded pulse train defined as

$$\chi(\lambda, f) = \int_{-\infty}^{\infty} u(\psi) u^*(\psi - \lambda) e^{j2\pi f \psi} d\psi = \sum_{l=1}^{N} \sum_{m=1}^{N} \boldsymbol{c}(l) \boldsymbol{c}^*(m) \chi_p[\lambda - (l-m)T_r, f],$$

The convex optimization MATLAB toolbox SeDuMi [26] is used for solving the SDP relaxation.

In Figure 2, the detection performance of the PCA-SC is plotted versus $|\alpha|^2$ with reference to the case of non-fluctuating target, $N = 16$, number of randomizations $L = 20$, several values of ϵ, and considering as similarity sequence a P3 code ([27] and [11, p. 127, 6.6]). For comparison, we also plot the P_d of the similarity code and the benchmark performance obtained maximizing the SNR without the constant modulus constraint, namely exploiting the optimal value of the problem

$$\begin{aligned} \max \quad & \boldsymbol{c}^\dagger \boldsymbol{R} \boldsymbol{c} \\ \text{s.t.} \quad & \|\boldsymbol{c}\|^2 = N. \end{aligned} \tag{15}$$

Of course, the considered benchmark performance is not in general achievable by a phase code, but it can be used to evaluate the performance loss that the constant modulus assumption implies

[7]We have also considered other values for the target normalized Doppler frequency. The results, not reported here, confirm the performance behavior showed in this section.

for $\epsilon = 2$. Finally, all the curves have been obtained averaging the results of $N_{exp} = 500$ statistically independent experiments. The results show that forcing stronger and stronger similarity constraints, we get worse and worse detection performances. This was actually expected since decreasing ϵ is tantamount to reducing the size of the feasible region. Moreover, this perfectly agrees with the behavior of the approximation bound which predicts worse and worse P_d decreasing ϵ. When $\epsilon = 0$, the performance ends up coincident with that of the similarity code which is the only feasible solution. The curves also highlight that the performance loss implied by the constant modulus assumption is a fraction of dB for $\epsilon = 2$.

The effects of the similarity constraint on the signal ambiguity function are analyzed in Figure 3. Therein, the modulus of $\chi(\lambda, f)$ is plotted exploiting the MATLAB toolbox of [28], under the assumption of rectangular pulses, $T_r = 5T_p$, and for several values of ϵ. The plots highlight that the closer ϵ to 0 the higher the degree of similarity between the ambiguity functions of the devised and the pre-fixed codes. This is due to the fact that decreasing ϵ is tantamount to reducing the size of the similarity region. In other words, we force the devised code to be more and more similar to the pre-fixed one and, as a consequence, we get more and more similar ambiguity functions.

The subsequent analysis is aimed at assessing the impact of the joint presence of both a strong and a weak scatterer on the performance achievable through the PSA-SC algorithm. To this end, we assume that a sidelobe scatterer, with complex amplitude α_s and zero-Doppler, is present in the received signal together with the useful target component (strong scatterer, whose Doppler frequency is also zero) and the disturbance component. The weak scatterer is located in the first sidelobe peak of the strong scatterer.

P3 and the codes whose ambiguity functions are given in Figures 3b-3d (which refer to three different values of the similarity parameter), have been considered. The P_d curves, versus $|\alpha|^2$, are plotted in Figure 4 for two values of the Target to Scatter power Ratio TSR$= 10 \log_{10}(|\alpha|^2/|\alpha_s|^2)$, i.e. TSR$= 10$ dB and TSR$= 30$ dB. The curves show that the presence of the weak scatterer reduces the detection capabilities of the codes.

In Figure 5, we study how the number of randomizations L affects the detection performance. We assume $N = 7$, similarity code equal to the Barker code $\boldsymbol{c}_0 = [1, 1, 1, -1, -1, 1, -1]^T$ of length 7, $\epsilon = 1.5$, and the remaining parameters equal to those of Figures 2 and 3. Therein

we also plot the curves corresponding to the benchmark performance, the Barker code, and the approximation bound, i.e.

$$P_d^{bound,c} = Q\left(\sqrt{2|\alpha|^2 R_c v(\text{SDP})}, \sqrt{-2\ln P_{fa}}\right).$$

Remarkably, with just 5-10 randomizations, we get a performance level very close to the curve obtained with 1000 random samples. In other words, the algorithm exhibits a very rapid convergence. Notice also that P_d of the PCA-SC is significantly superior than that corresponding to the approximation bound. This behavior can be explained observing that the quoted bound is based on a worst case analysis and it often happens in practice that the actual performance is substantially better than the worst case. A similar behavior was also found in [14] with reference to multiuser detection.

The detection performance of the FA-PCA-SC is studied in Figure 6 where P_d is plotted versus $|\alpha^2|$ for $M = 16$, several values of ϵ, and the remaining simulation parameters equal to those of Figure 2. Therein the benchmark P_d and that obtained using the P3 code are reported too. It is interesting to observe that the performance of the considered technique does not show a continuous variation with the parameter ϵ as it happens for the PCA-SC case. Actually, it exhibits jumps and the actual P_d curve depends on the specific interval where the parameter ϵ lies. Otherwise stated, all the ϵ values which belong to the interval $\mathcal{I}_i$, $i = 0, \ldots, M/2-1$, defined as

$$\mathcal{I}_i = [\epsilon_i, \epsilon_{i+1}), \qquad \epsilon_i = \sqrt{2\left(1 - \cos\left(\frac{2\pi}{M} i\right)\right)}, \qquad i\text{-th } \epsilon\text{-interval},$$

lead to the same performance curve (i.e. the corresponding P_d curves perfectly overlap). This behavior can be explained observing that the values of the similarity parameter which lie in the same ϵ-interval lead to the same feasible region and the same approximation bound. The plots also show that, given two separated ϵ-intervals, the one with the largest second extreme contains values of ϵ providing the highest P_d.

However, this improvement in the detection performance is accompained by a deterioration of the coded pulse train ambiguity function. This is shown in Figure 7 where such function is plotted assuming rectangular pulses, $T_r = 5T_p$, and for some values of ϵ which belong to different ϵ-intervals.

The effects of the number of randomizations on the FA-PCA-SC performance is analyzed in Figure 8, where P_d is plotted versus $|\alpha|^2$ for several values of L, $M = 4$, and with the other simulation parameters equal to those of Figure 5. For comparison purposes, we also plot the benchmark performance, the P_d obtained resorting to an optimal solution of (13) computed through an exhaustive search, the Barker code P_d, and the P_d predicted by the approximation bound, i.e.

$$P_d^{bound,d} = Q\left(\sqrt{2|\alpha|^2 R_d v(\text{SDP})}, \sqrt{-2\ln P_{fa}}\right).$$

Again, the curves show a rapidly convergent behavior; 5-10 randomizations are sufficient to get a performance level very close to that obtained through the exhaustive search. Moreover, P_d of the FA-PCA-SC is significantly superior than that predicted by the approximation bound.

VII. Conclusions

In this paper, we have considered the design of radar phase codes which optimize the detection performance under a similarity constraint with a given sequence which exhibits a desirable ambiguity function. We have considered the cases of both continuous and finite code alphabet and have formulated the code design in terms of non-convex quadratic optimization problems. Due to the NP-hard nature of the problems, we have focused on techniques capable of approximating the optimal solution in polynomial time. Precisely, we have devised two coding algorithms which are based on the theory of SDP relaxation and randomization. Remarkably, in both cases we have derived the approximation bounds which characterize the quality of the produced solutions.

At the analysis stage, we have assessed the performance of the new coding schemes both in terms of detection probability and ambiguity function. The results have highlighted that it is possible to realize a trade off between the actual detection performance and the shape of the pulse train ambiguity function. Moreover, the new encoding techniques require a quite modest number of randomizations to provide a satisfactory performance level.

Possible future research tracks might concern the possibility to make the algorithms adaptive with respect to the disturbance covariance matrix, namely to devise techniques which jointly estimate the code and the covariance. The introduction of knowledge-based constraints should also be investigated in the code design optimization problem, as well as the extension of the framework to the challenging MIMO radar case. Before concluding, we explicitly notice that it

is possible to generalize the mathematical framework considered in this paper to a more general class of constraints accounting for a possibly different similarity parameter on each entry of the code.

ACKNOWLEDGEMENTS

The authors would like to thank the Associate Editor, Dr. D. P. Palomar, and the anonymous Reviewers for the helpful comments toward the improvement of this paper.

VIII. Appendix A: Proof of Proposition 4.2

Proof. We have $f(x) = \frac{\sqrt{2-2\cos x}}{2\pi - x} = \frac{2\sin(x/2)}{2\pi - x}$ for $x \in [0, 2\pi]$. It is easily verified that $f(0) = 0$ and $f(2\pi) = 1$. Now we wish to show that $f(x) = \frac{2\sin(x/2)}{2\pi - x}$ is strictly increasing over $(0, 2\pi)$. It is easily seen that $f'(x) = \frac{2\sin(x/2) + \cos(x/2)(2\pi - x)}{(2\pi - x)^2}$. When $x \in (0, \pi]$, $f'(x) > 0$; when $x \in (\pi, 2\pi)$, $f'(x) > 0 \Leftrightarrow 2\sin(x/2) + \cos(x/2)(2\pi - x) > 0 \Leftrightarrow -\tan(x/2) \geq \pi - x/2 \Leftrightarrow \tan s > s$ for $s \in (0, \pi/2)$, which is a known inequality. □

IX. Appendix B: Proof of Proposition 5.2

Proof. Clearly we have $f(1) = 0$, and $f(M) = 2M\sin(\pi\frac{1}{M}) > 0$, due to $M \geq 3$. It is essential to prove that $f(x)$ is strictly increasing over the interval $1 < x < M$. To this end, we set $f(x) := f(x)/2$, and check its derivative:

$$f'(x) = \frac{\pi}{Mx^2 \sin^2(\pi(\frac{1}{x} - \frac{1}{M}))} \left(x^2 \cos(\pi\frac{x}{M}) \sin(\pi\frac{1}{x}) \sin(\pi(\frac{1}{x} - \frac{1}{M})) + M \sin(\pi\frac{x}{M}) \sin(\pi\frac{1}{M}) \right).$$

Since $1 > \frac{1}{x} > \frac{1}{x} - \frac{1}{M} > 0$ and $1 > \frac{x}{M} > \frac{1}{M}$, it is seen that $f'(x) > 0$ for $1 < x \leq \frac{M}{2}$, and then $f(x)$ is strictly increasing over $(1, \frac{M}{2}]$. Notice that

$$f'(x) = \frac{\pi \cos(\pi\frac{x}{M})}{Mx^2 \sin^2(\pi(\frac{1}{x} - \frac{1}{M}))} \left(x^2 \sin(\pi\frac{1}{x}) \sin(\pi(\frac{1}{x} - \frac{1}{M})) + M \tan(\pi\frac{x}{M}) \sin(\pi\frac{1}{M}) \right), x \in (\frac{M}{2}, M).$$

To prove $f'(x) > 0$ for $\frac{M}{2} < x < M$, it suffices to show that

$$g(x) := x^2 \sin(\pi\frac{1}{x}) \sin(\pi(\frac{1}{x} - \frac{1}{M})) + M \tan(\pi\frac{x}{M}) \sin(\pi\frac{1}{M}) < 0, x \in (\frac{M}{2}, M)$$

Observe that $\tan(x) < x - \pi$ for $\frac{\pi}{2} < x < \pi$. Then

$$\begin{aligned} g(x) &< x^2 \sin(\pi\frac{1}{x}) \sin(\pi(\frac{1}{x} - \frac{1}{M})) + M(\pi\frac{x}{M} - \pi) \sin(\pi\frac{1}{M}) \\ &= x^2 \sin(\pi\frac{1}{x}) \sin(\pi(\frac{1}{x} - \frac{1}{M})) - (M - x)\pi \sin(\pi\frac{1}{M}) \\ &< x^2 \sin(\pi\frac{1}{x})(\pi(\frac{1}{x} - \frac{1}{M})) - (M - x)\pi \sin(\pi\frac{1}{M}), \end{aligned}$$

where in the last inequality we have used the fact $\sin x < x$ for $x \in (0, \pi)$, and it further suffices to show

$$x^2 \sin(\pi\frac{1}{x})(\pi(\frac{1}{x} - \frac{1}{M})) < (M - x)\pi \sin(\pi\frac{1}{M}), \ \frac{M}{2} < x < M,$$

or equivalently,

$$x \sin(\pi\frac{1}{x}) < M \sin(\pi\frac{1}{M}), \ \frac{M}{2} < x < M.$$

However, this immediately follows from the observation that the function $x \sin(\frac{\pi}{x})$ is strictly increasing over $(\frac{M}{2}, M)$ for any given $M \geq 2$. The proposition is thus proved. □

REFERENCES

[1] A. Farina, "Waveform Diversity: Past, Present, and Future", *Third International Waveform Diversity & Design Conference*, Plenary Talk, Pisa, June 2007.

[2] Special issue on "Adaptive Waveform Design for Agile Sensing and Communications", Edited by A. Nehorai, F. Gini, M. S. Greco, A. Papandreou-Suppappola, and M. Rangaswamy, *IEEE Journal on Selected Topics in Signal Processing*, Vol. 1, No. 1, pp. 2-213.

[3] J. S. Bergin, P. M. Techau, J. E. Don Carlos, and J. R. Guerci, "Radar Waveform Optimization for Colored Noise Mitigation", *2005 IEEE International Radar Conference*, pp. 149-154, Alexandria, VA, 9-12 May 2005.

[4] J. Li, J. R. Guerci, and L. Xu, "Signal Waveform's Optimal-under-Restriction Design for Active Sensing", *IEEE Signal Processing Letters*, Vol. 13, No. 9, pp. 565-568, September 2006.

[5] B. Friedlander, "A Subspace Framework for Adaptive Radar Waveform Design ", *Record of the Thirty-Ninth Asilomar Conference on Signals, Systems and Computers 2005*, Pacific Grove, CA, pp. 1135-1139, October 28 - November 1, 2005.

[6] D. T. Gjessing, *Target Adaptive Matched Illumination Radar Principles and Applications*, IEE Electromagnetic Wave Series, London, U.K., Peter Peregrinus, 1986.

[7] A. Farina and F. A. Studer, "Detection with High Resolution Radar: Great Promise, Big Challenge", *Microwave Journal*, pp. 263-273, May 1991.

[8] S. U. Pillai, H. S. Oh, D. C. Youla, and J. R. Guerci, "Optimum Transmit-Receiver Design in the Presence of Signal-Dependent Interference and Channel Noise", *IEEE Transactions on Information Theory*, Vol. 46, No. 2, pp. 577-584, March 2000.

[9] D. A. Garren, A. C. Odom, M. K. Osborn, J. S. Goldstein, S. U. Pillai, and J. R. Guerci, "Full-Polarization Matched-Illumination for Target Detection and Identification", *IEEE Transactions on Aerospace and Electronic Systems*, Vol. 38, No. 3, pp. 824-837, July 2002.

[10] S. Kay, "Optimal Signal Design for Detection of Point Targets in Stationary Gaussian Clutter/Reverberation", *IEEE Journal on Selected Topics in Signal Processing*, Vol. 1, No. 1, pp. 31-41, June 2007.

[11] N. Levanon and E. Mozeson, *Radar Signals*, John Wiley & Sons, 2004.

[12] M. Bell, "Information Theory of Radar and Sonar Waveforms", *Wiley Encyclopedia of Electrical and Electronic Engineering*, J. G. Webster, Ed., Vol. 10, pp. 180-190, New York, NY: Wiley-Interscience, 1999.

[13] A. De Maio, S. De Nicola, Y. Huang, S. Zhang, and A. Farina, "Code Design to Optimize Radar Detection Performance under Accuracy and Similarity Constraints", submitted to *IEEE Transactions on Signal Processing*, August 2007.

[14] Wing-Kin Ma, T. N. Davidson, Kon Max Wong, Zhi-Quan Luo, and Pak-Chung Ching, "Quasi-Maximum-Likelihood Multiuser Detection Using Semi-Definite Relaxation with Application to Synchronous CDMA", *IEEE Transactions on Signal Processing*, Vol. 50, No. 4, pp. 912 - 922, April 2002.

[15] A. Mobasher, M. Taherzadeh, R. Sotirov, and A. K. Khandani, "A Near-Maximum-Likelihood Decoding Algorithm for MIMO Systems Based on Semi-Definite Programming", *IEEE Transactions on Information Theory*, Vol. 53, No. 11, pp. 3869 - 3886, November 2007.

[16] E. Karipidis, N. D. Sidiropoulos, Zhi-Quan Luo, "Convex Transmit Beamforming for Downlink Multicasting to Multiple Co-Channel Groups", *Proceedings of the 2006 IEEE International Conference on Acoustics, Speech and Signal Processing*, Vol. 5, 14-19 May 2006.

[17] R. A. Horn and C. R. Johnson, *Matrix Analysis*, Cambridge University Press, 1985.

[18] J. S. Goldstein, I. S. Reed, and P. A. Zulch, "Multistage Partially Adaptive STAP CFAR Detection Algorithm", *IEEE Transactions on Aerospace and Electronic Systems*, Vol. 35, No. 2, pp. 645-661, April 1999.

[19] H. L. Van Trees, *Optimum Array Processing. Part IV of Detection, Estimation, and Modulation Theory*, John Wiley & Sons, 2002.

[20] N.D. Sidiropoulos, T.N. Davidson, and Zhi-Quan Luo, "Transmit Beamforming for Physical-Layer Multicasting", *IEEE Transactions on Signal Processing*, Vol. 54, No. 6, pp. 2239 - 2251, June 2006.

[21] S. Zhang and Y. Huang, "Complex Quadratic Optimization and Semidefinite Programming", *SIAM Journal on Optimization*, Vol. 16, No. 3, pp. 871 - 890, 2006.

[22] A. So, J. Zhang, and Y. Ye, "On Approximating Complex Quadratic Optimization Problems Via Semidefinite Programming Relaxations", *Mathematical Programming*, Series B, Vol. 110, No. 1, pp. 93 - 110, June 2007.

[23] G. H. Golub and C. F. Van Loan, *Matrix Computations*, Johns Hopkins Series in the Mathematical Sciences, third edition, 1996.

[24] A. Frieze and M. Jerrum, "Improved Approximation Algorithms for MAX k-CUT and MAX BISECTION", *Algorithmica*, Vol. 18, No. 1, pp. 67 - 81, May 1997.

[25] M. X. Goemans and D. P. Williamson, "Approximation Algorithms for MAX-3-CUT and Other Problems Via Complex Semidefinite Programming", *Journal of Computer and System Sciences*, Vol. 68, No. 2, pp. 442 - 470, March 2004.

[26] J. F. Sturm, "Using SeDuMi 1.02, a MATLAB Toolbox for Optimization over Symmetric Cones", *Optimization Methods and Software*, Vol. 11-12, pp. 625-653, August 1999.

[27] F. F. Kretschmer and B. L. Lewis, "Doppler Properties of Polyphase Coded Pulse Compression Waveforms", *IEEE Transactions on Aerospace and Electronic Systems*, Vol. 19, No. 4, pp. 521-531, July 1983.

[28] E. Mozeson and N. Levanon, "MATLAB Code for Plotting Ambiguity Functions", *IEEE Transactions on Aerospace and Electronic Systems*, Vol. 38, No. 3, pp. 1064-1068, July 2002.

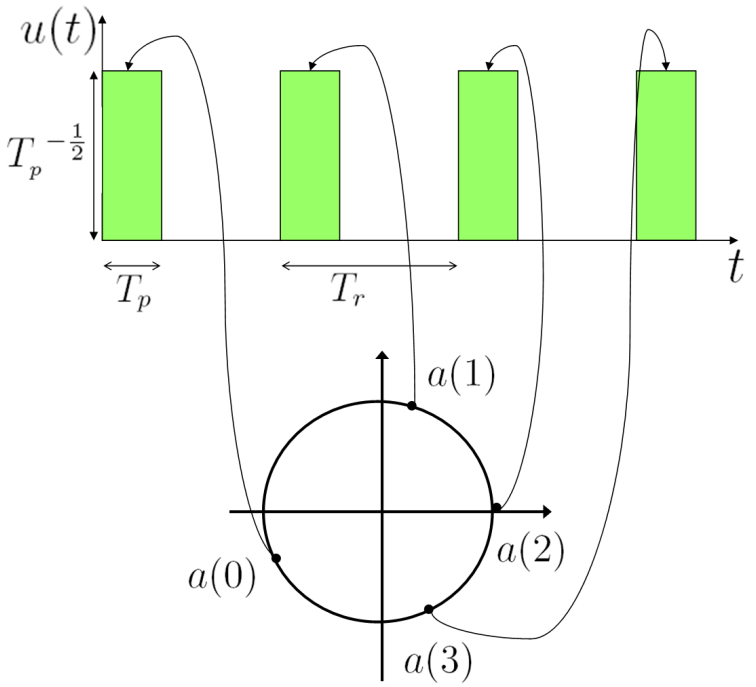

Figure 1: Phase coded pulse train $u(t)$ for $N = 4$, $T_r = 3T_p$ and $p(t)$ with rectangular shape.

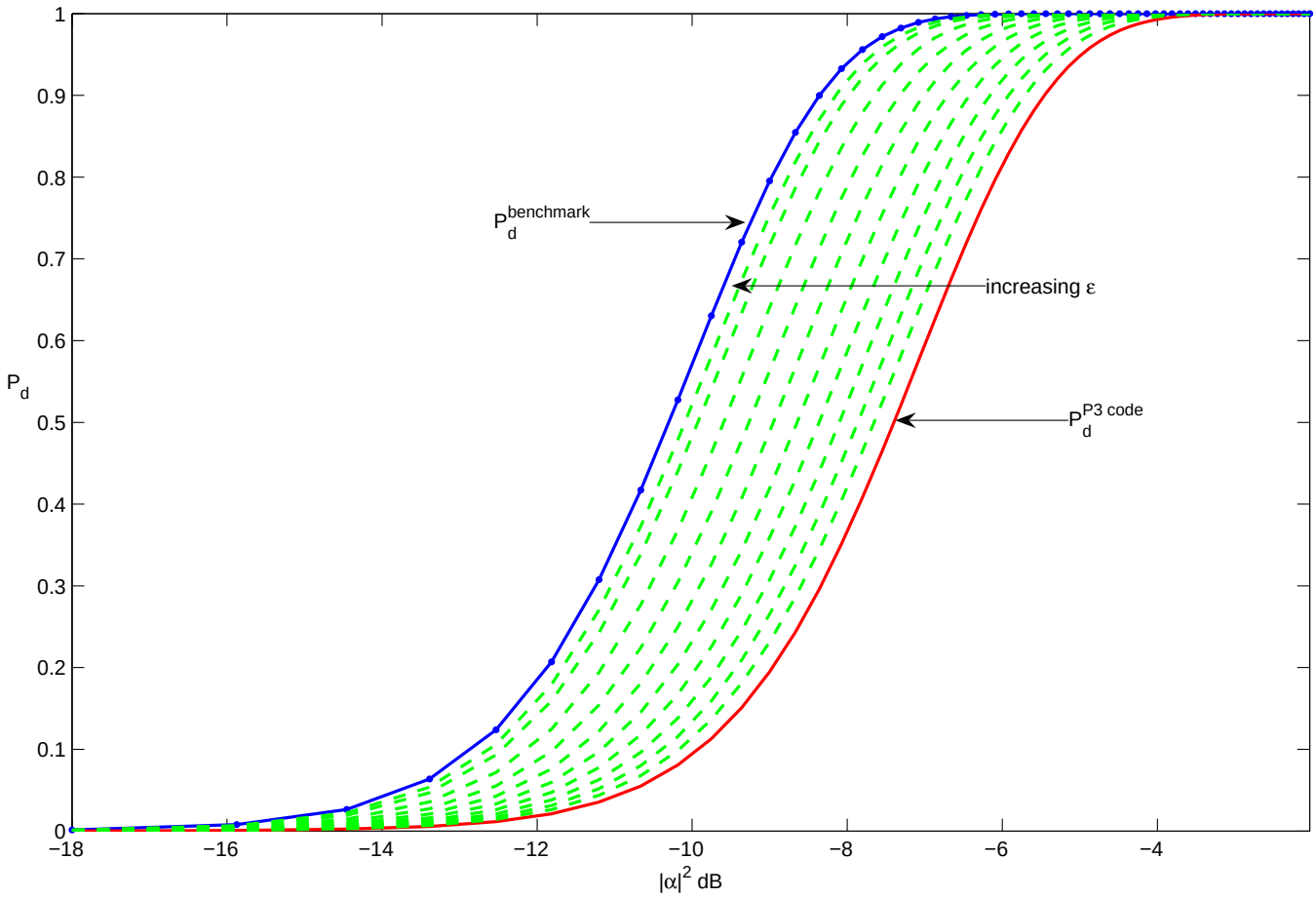

Figure 2: P_d of PCA-SC versus $|\alpha|^2$ (dashed curves) for $P_{fa} = 10^{-6}$, non-fluctuating target, $N = 16$, $L = 20$, similarity code P3, and several values of $\epsilon \in \{0, 0.3, 0.5, 0.7, 0.9, 1.1, 1.3, 1.5, 1.7, 1.9, 2.0\}$. $P_d^{benchmark}$ (dotted-marked curve). $P_d^{P3\ code}$ (solid curve). Notice that, for $\epsilon = 0$, P_d perfectly overlaps with $P_d^{P3\ code}$.

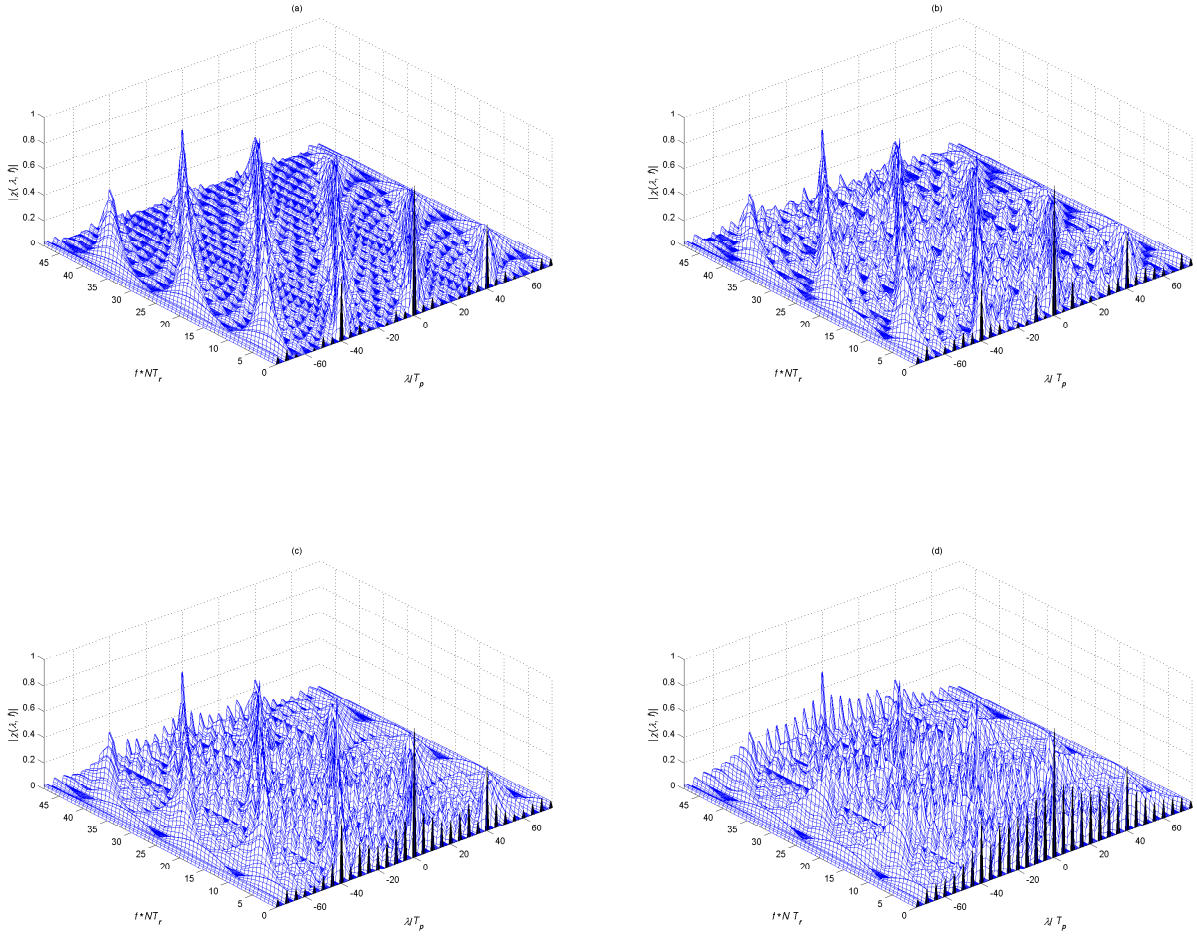

Figures 3a-3d: Ambiguity function modulus of PCA-SC for $N = 16$, $L = 20$, $T_r = 5T_p$, similarity code P3, and several values of ϵ: (a) $\epsilon = 0$, (b) $\epsilon = 0.5$, (c) $\epsilon = 1.0$, (d) $\epsilon = 1.5$.

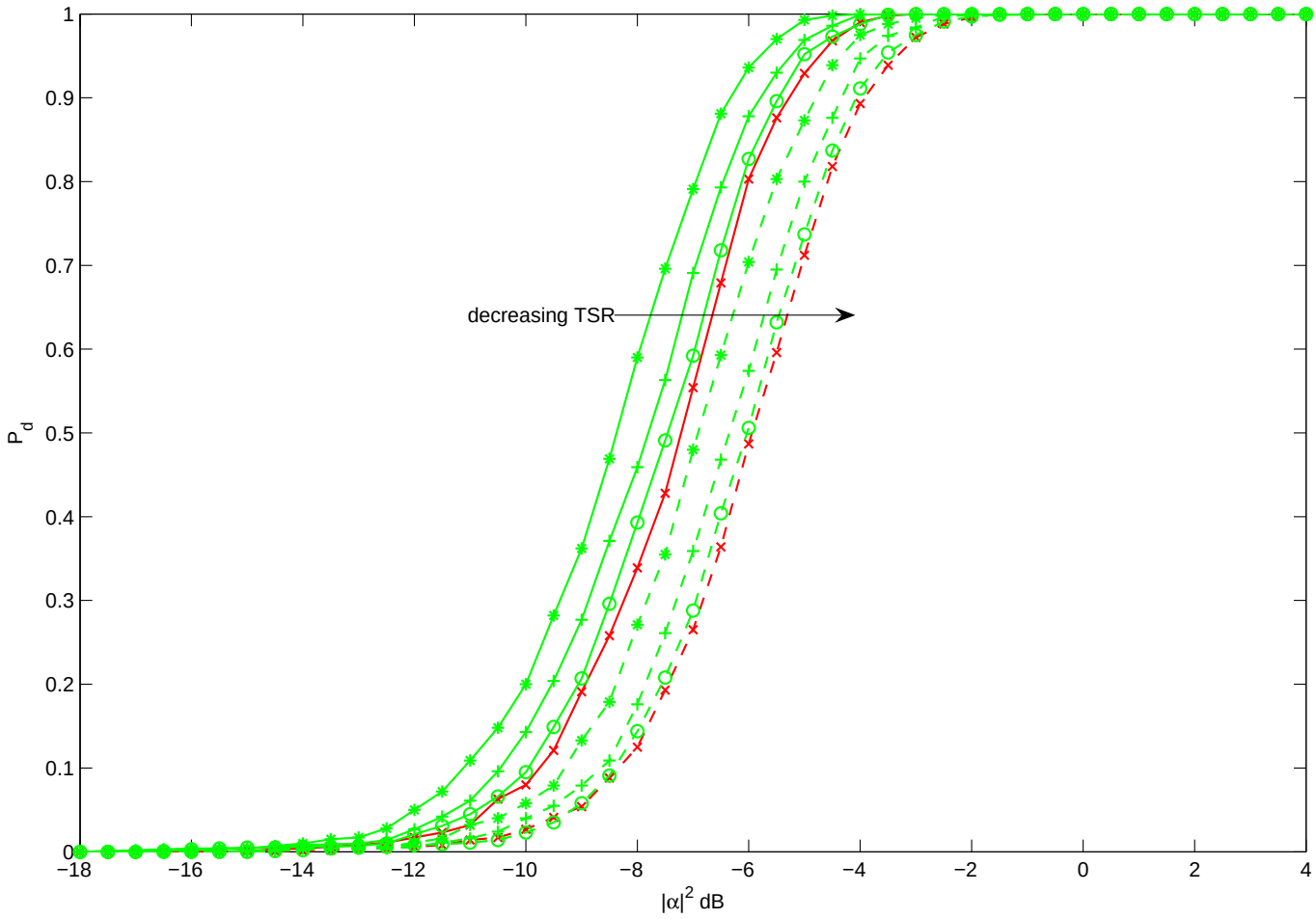

Figure 4: P_d of PCA-SC versus $|\alpha|^2$ for $P_{fa} = 10^{-6}$, non-fluctuating target, $N = 16$, $L = 20$, similarity code P3, and two values of TSR, TSR=10 dB (dashed curves) and TSR=30 dB (solid curves). P3 code (x-marked curves). Code whose ambiguity function is in Figure 3b (o-marked curves). Code whose ambiguity function is in Figure 3c (plus-marked curves). Code whose ambiguity function is in Figure 3d (asterisk-marked curves).

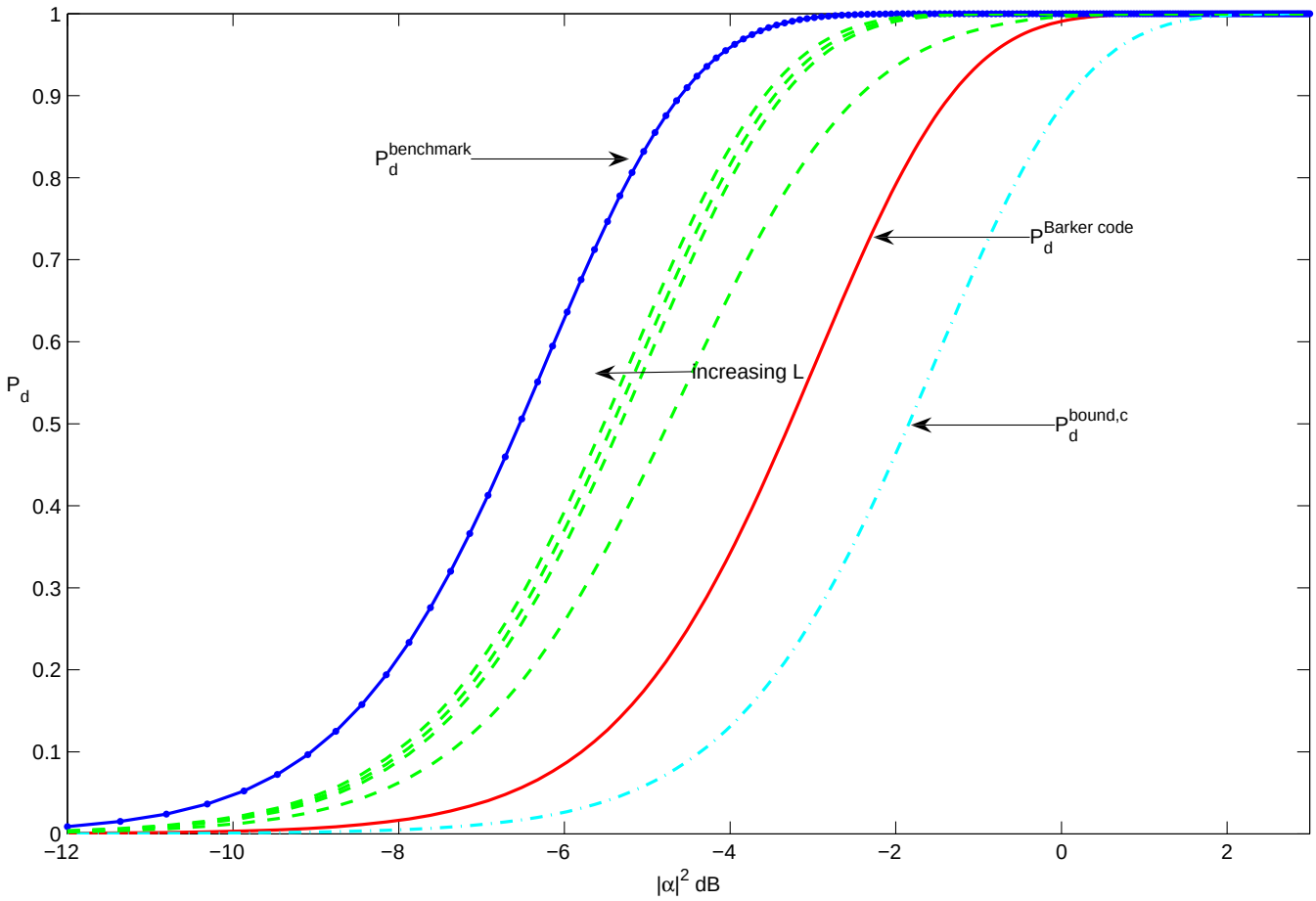

Figure 5: P_d of PCA-SC versus $|\alpha|^2$ (dashed curves) for $P_{fa} = 10^{-6}$, non-fluctuating target, $N = 7$, $\epsilon = 1.5$, similarity code Barker, and several values of $L \in \{1, 5, 10, 1000\}$. $P_d^{benchmark}$ (dotted-marked curve). $P_d^{Barker\ code}$ (solid curve). $P_d^{bound,c}$ (dash-dotted curve).

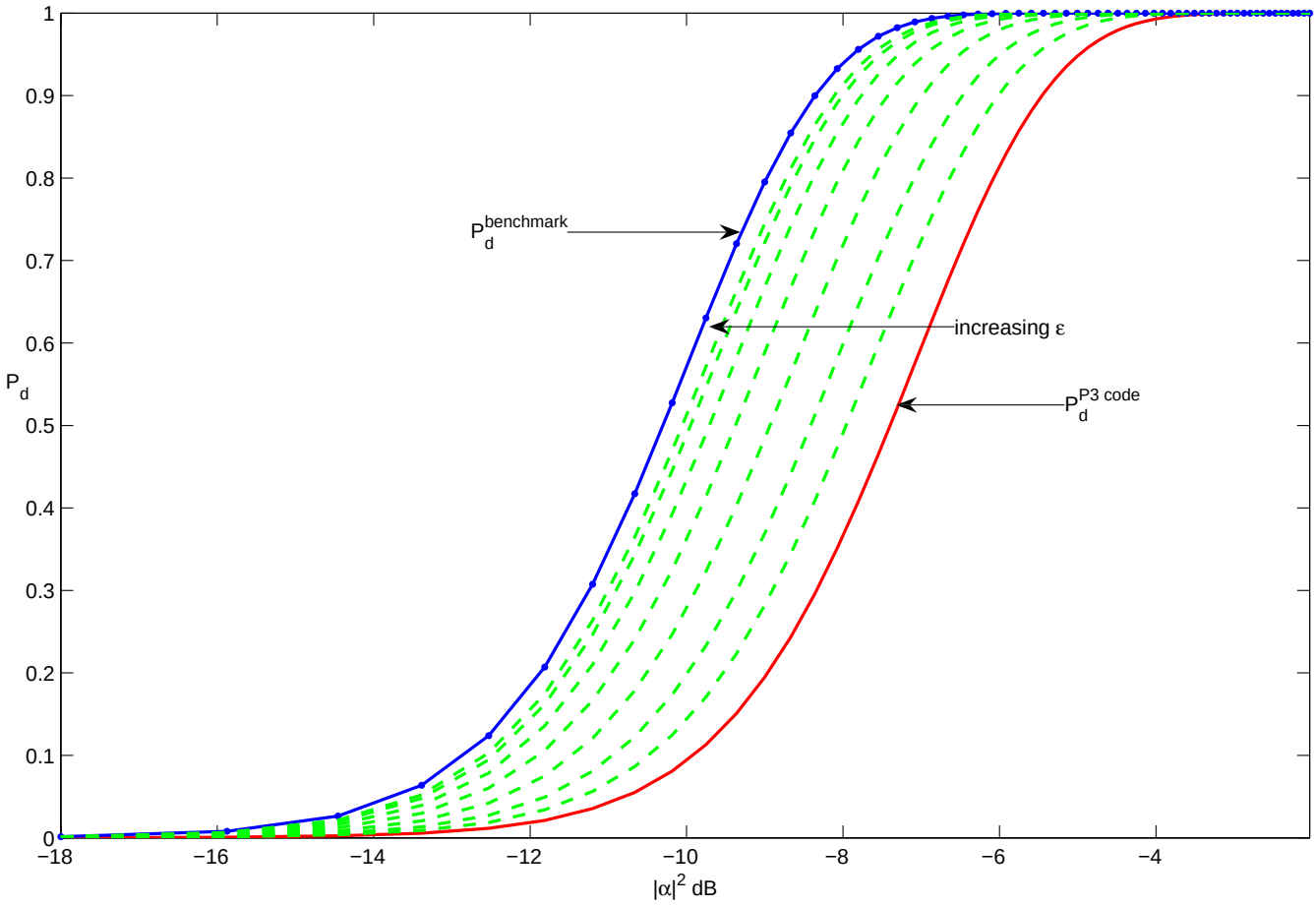

Figure 6: P_d of FA-PCA-SC versus $|\alpha|^2$ (dashed curves) for $P_{fa} = 10^{-6}$, non-fluctuating target, $N = 16$, $M = 16$, $L = 20$, similarity code P3, and several values of $\epsilon \in \{0.1951, 0.5778, 0.9383, 1.2627, 1.5386, 1.7553, 1.9047, 1.98080\}$. $P_d^{benchmark}$ (dotted-marked curve). $P_d^{P3\ code}$ (solid curve). Notice that, for $\epsilon \in \left[0, \sqrt{2(1-\cos\frac{2\pi}{M})}\right)$, P_d perfectly overlaps with $P_d^{P3\ code}$.

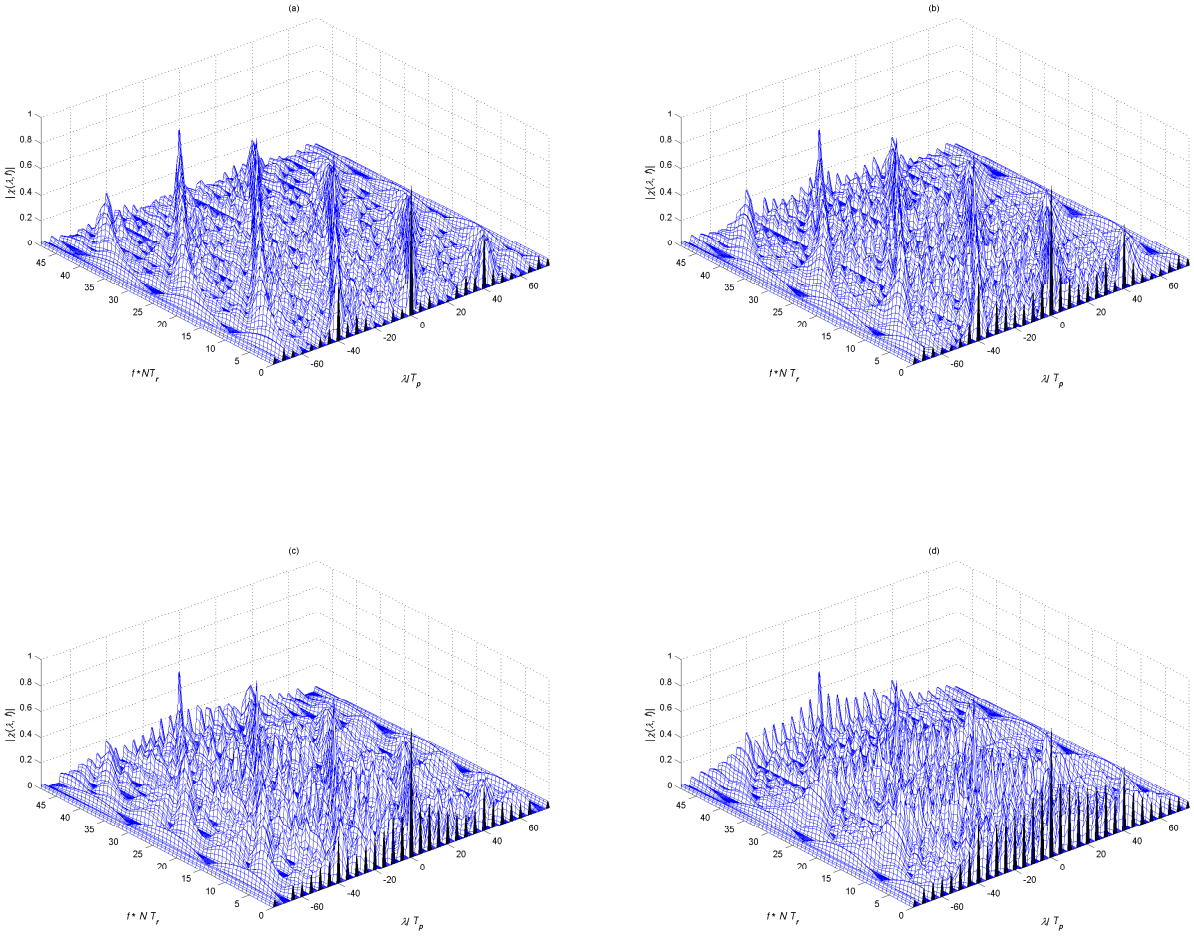

Figures 7a-7d: Ambiguity function modulus of FA-PSC-SC for $N = 16$, $L = 20$, $T_r = 5T_p$, similarity code P3, and several values of ϵ: (a) $\epsilon = 0.5778$, (b) $\epsilon = 0.9383$, (c) $\epsilon = 1.2627$, (d) $\epsilon = 1.5386$.

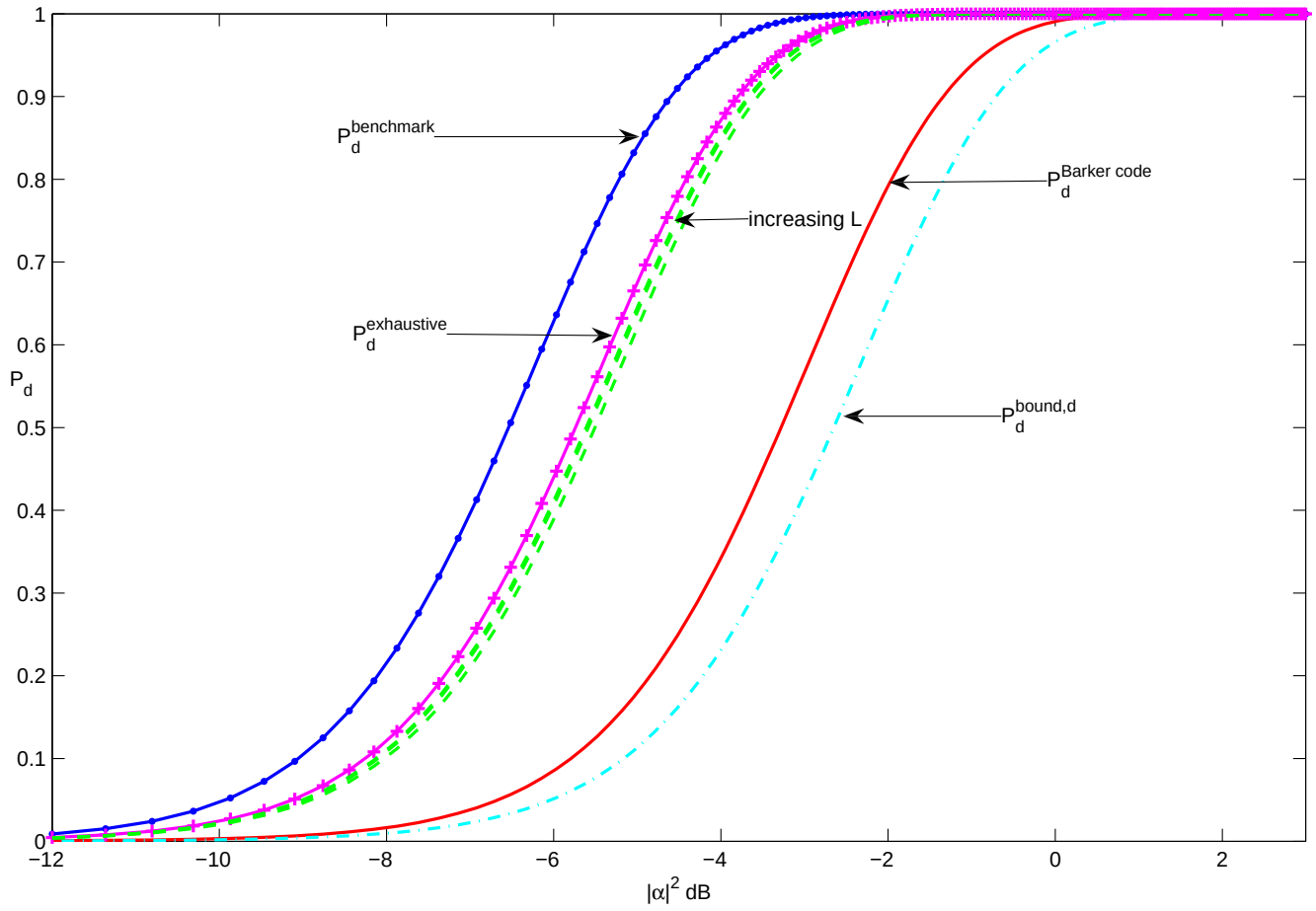

Figure 8: P_d of FA-PCA-SC versus $|\alpha|^2$ (dashed curves) for $P_{fa} = 10^{-6}$, non-fluctuating target, $N = 7$, $\epsilon = 1.5$, similarity code Barker, and several values of $L \in \{1, 5, 10\}$. $P_d^{benchmark}$ (dotted-marked curve). $P_d^{Barker\ code}$ (solid curve). $P_d^{bound,c}$ (dash-dotted curve). $P_d^{exhaustive}$ (plus-marked curve).